Development/Plasticity/Repair

Alteration of Gene Expression by Chromosome Loss in the Postnatal Mouse Brain

Dhruv Kaushal,[1,3] James J. A. Contos,[3] Kai Treuner,[5] Amy H. Yang,[2,3] Marcy A. Kingsbury,[3] Stevens K. Rehen,[3] Michael J. McConnell,[2,3,5] Masaru Okabe,[4] Carrolee Barlow,[5] and Jerold Chun[1,2,3]

[1]Neuroscience and [2]Biomedical Sciences Programs, and [3]Department of Pharmacology, University of California, San Diego, San Diego, California 92093, [4]Genome Information Research Center, Osaka University, Suita, Osaka, 565-0871 Japan, [5]Laboratory of Genetics, The Salk Institute for Biological Studies, La Jolla, California 92037

Frequent chromosomal aneuploidy has recently been discovered in normal neurons of the developing and mature murine CNS. Toward a more detailed understanding of aneuploidy and its effects on normal CNS cells, we examined the genomes of cells in the postnatal subventricular zone (SVZ), an area that harbors a large number of neural stem and progenitor cells (NPCs), which give rise to neurons and glia. Here we show that NPCs, neurons, and glia from the SVZ are frequently aneuploid. Karyotyping revealed that ~33% of mitotic SVZ cells lost or gained chromosomes *in vivo*, whereas interphase fluorescence *in situ* hybridization demonstrated aneuploidy in postnatal-born cells in the olfactory bulb (OB) *in vivo*, along with neurons, glia, and NPCs *in vitro*. One possible consequence of aneuploidy is altered gene expression through loss of heterozygosity (LOH). This was examined in a model of LOH: loss of transgene expression in mice hemizygous for a ubiquitously expressed enhanced green fluorescent protein (eGFP) transgene on chromosome 15. Concurrent examination of eGFP expression, transgene abundance, and chromosome 15 copy number demonstrated that a preponderance of living SVZ and OB cells not expressing eGFP lost one copy of chromosome 15; the eGFP transgene was lost in these cells as well. Although gene expression profiling revealed changes in expression levels of several genes relative to GFP-expressing controls, cells with LOH at chromosome 15 were morphologically normal and proliferated or underwent apoptosis at rates similar to those of euploid cells *in vitro*. These findings support the view that NPCs and postnatal-born neurons and glia can be aneuploid *in vivo* and functional gene expression can be permanently altered in living neural cells by chromosomal aneuploidy.

Key words: **stem cells; aneuploidy; loss of heterozygosity; mosaicism; olfactory bulb; gene expression profiling**

Introduction

Rapid division of stem and progenitor cells during CNS development gives rise to the neurons and glia that populate the adult brain. Faithful transmission of genetic information during these divisions is thought to be essential for normal brain development, but until recently the fidelity of transmission of genetic information during CNS development had not been measured.

We recently examined the genomes of developing and mature neurons of the mouse cerebral cortex and made the surprising discovery that 33% of proliferating cortical stem and progenitor cells became aneuploid (i.e., lost or gained one or more whole chromosomes), in part through chromosome mis-segregation during mitosis (Rehen et al., 2001). Many, but not all, aneuploid cells appeared to survive as neurons in the adult cerebral cortex.

Is the genesis of aneuploid cells restricted to the cerebral cortex? Does aneuploidy alter gene expression, survival, or proliferation of neural cells? To address these questions, we studied aneuploidy and its effects on gene expression and function in normal neural cells from the subventricular zone (SVZ) of the postnatal mouse brain. The SVZ is one of two neurogenic areas in the mammalian CNS that remains active throughout life (Gage, 2002) via proliferation of a pool of neural progenitor cells (NPCs) (Alvarez-Buylla and Garcia-Verdugo, 2002). The cells of the SVZ have been well characterized, with an eye toward their potential therapeutic uses (Aboody et al., 2000). We used the SVZ as a model because of its accessibility and relative homogeneity (Doetsch et al., 1997), which allowed us to (1) characterize the extent of aneuploidy and identify aneuploid cells, and (2) directly examine the effects of aneuploidy on gene expression, proliferation, and survival.

Materials and Methods

Metaphase chromosome spreads. Chromosome spreads were obtained from mitotic SVZ or embryonic liver cells using standard protocols (Barch et al., 1997; Rehen et al., 2001). Briefly, postnatal day (P) 5 to P10 SVZs were dissected and held intact for 3–5 hr in Opti-Mem supple-

Received Aug. 28, 2002; revised April 4, 2003; accepted April 7, 2003.

This work was supported by an unrestricted gift from Merck (J.C.), predoctoral funding from the Pharmaceutical Research and Manufacturers Association foundation (D.K.) and National Institute of General Medical Sciences (M.J.M. and A.H.Y.), and postdoctoral funding from the Pew Foundation (S.K.R.) and National Institute of Mental Health (M.A.K.).We thank Dr. Fred Gage for critical reading of this manuscript and helpful discussions. We are grateful to Marisa Fontanoz, Grace Kennedy, and Carol Akita for technical assistance, and Dennis Young and the University of California, San Diego flow cytometry shared resource for flow sorting.

Correspondence should be addressed to Dr. Jerold Chun, Department of Molecular Biology, The Scripps Research Institute, 10550 North Torrey Pines Road, ICND-118, La Jolla, CA 92037. E-mail: jchun@scripps.edu.

D. Kaushal's, A. Yang's, M. Kingsbury's, S. Rehen's, and M. McConnell's present address: Department of Molecular Biology, The Scripps Research Institute, La Jolla, CA 92037.

J. Contos' present address: Fred Hutchinson Cancer Research Center, Seattle, WA 98109.

C. Barlow's present address: Merck Research Labs, San Diego, CA 92121.

 0270-6474/03/235599-08$15.00/0

mented with 10 ng/ml FGF-2 and 100 ng/ml colcemid (Invitrogen, San Diego, CA) to arrest cells in metaphase. Individual cells were then dissociated and incubated in 75 mM KCl for 12–15 min before fixation in 3:1 methanol:acetic acid. Embryonic day (E) 13 livers were dissected from contaminating mesoderm and gut before arrest and fixation as described above.

In situ *hybridization.* Hybridizations of metaphase chromosome spreads were performed using mouse Spectral Karyotyping (SKY) paints (Applied Spectral Imaging, Carlsbad, CA) according to manufacturer instructions. Hybridizations of interphase nuclei or cultured cells with mouse whole chromosome paints (Applied Spectral Imaging) were performed as described previously (Rehen et al., 2001). Error rates for SKY and interphase fluorescence *in situ* hybridization (FISH) karyotypes were estimated to be <2% in previous studies in which rates of chromosome loss measured by interphase FISH or SKY were compared with rates estimated from direct measurement of DNA content (Rehen et al., 2001).

Cell culture. Culture of SVZ cells for FISH was performed by the methods of Lim and Alvarez-Buylla (1999) or Reynolds et al. (1992) with the following modifications: cells were cultured in Opti-Mem (Invitrogen) supplemented with 2.5% fetal calf serum and/or 10 ng/ml FGF-2 and 20 ng/ml epidermal growth factor (EGF). For FISH analysis, cells were dispersed onto poly-lysine-coated dishes (Sigma, St. Louis, MO) or slides after brief incubation and mild trituration in PBS with 2 mM EGTA. For flow-sorting and gene expression profiling or antibody staining, SVZ glia and glial-restricted NPCs were expanded in Opti-Mem containing 2.5% serum, EGF, and FGF-2 (Levison and Goldman, 1997) for 10 d before fluorescence-activated cell sorting (FACS). For antibody staining after flow sorting, cells were harvested by centrifugation for 10 min at 500 × *g*, resuspended in 50–100 μl of Opti-Mem, and plated onto 12 mm coverslips (Fisher Scientific, Pittsburgh, PA) coated with cell-tak (Collaborative Research, Bedford, MA) or poly-lysine (Sigma) as described previously (Fukushima et al., 1998).

Flow sorting. Cells from green fluorescent protein (GFP) transgenic mice were sorted by standard protocols (Kawakami et al., 1999) in PBS supplemented with 2% bovine serum albumin (Sigma). GFP+ and GFP− cells were isolated first by establishing suitable gates for live cells on the basis of forward and side light scatter, GFP peak width, and exclusion of propidium iodide (Sigma), and then sorted into GFP+ and GFP− bins on the basis of GFP intensity. After sorting, cells were either cultured for 12–24 hr and stained with antibodies or harvested for isolation of genomic DNA or total RNA.

PCR. Genomic DNA was isolated by standard protocols with the exception that in the FACS-sorted cells (because of low genomic DNA quantities), 10 μg of yeast tRNA was used as a carrier to precipitate the DNA. The amount of genomic DNA (gDNA) in the samples was estimated on the basis of cell counts from FACS. PCR reactions of 20 μl consisted of 1 PCR buffer (Invitrogen), 2 mM $MgSO_4$, 0.25 mM each dNTP, 0.5 mM each primer, and 0.5 U HiFi *Taq* (Invitrogen). Tubes were cycled 35 times (95°C for 30 sec; 56°C for 30 sec; 72°C for 3 min). Primer pairs used for *s1p3* were edg3a (5′-CGCATGTACTTTTTCATTGGCAA-3′) and edg3c (5′-GGGTTCATGGCGGAGTTGAG-3′), and for GFP, eGFPF2 (5′-GGCAAGCTGACCCTGAAGTT-3′) and eGFPR3 (5′-GCGCTTCTCGTTGGGGTCTTT-3′). Expected PCR product sizes were 528 bp (eGFPF2–eGFPR3) and 627 bp (edg3a–edg3c). Products were separated and visualized by electrophoresis on 1.2% agarose gels containing 0.5 μg/ml ethidium bromide. Gels were also Southern blotted and probed with fragments of the corresponding gene. Products were quantitated using a densitometer.

The other primer pair used to amplify the GFP gene gave a PCR product of 645 bp using eGFPF1 (5′-CGA CGT AAA CGG CCA CAA GTT-3′) and eGFPR1 (5′-TCG TCC ATG CCG AGA GTG AT-3′). We also amplified *s1p2* from chromosome 9 (expected product size, 415 bp; using edg4a 5′-TTA ACT CCC GTG CAG TGG TTT GC-3′ and edg4b 5′-ACG ATG GTG ACC GTC TTG AGC A-3′).

Gene expression profiling. Three separate paired GFP+ and GFP− SVZ cell samples were sorted into RNA-Later (Ambion, Austin, TX), and RNA was isolated using a StrataPrep total RNA isolation kit (Stratagene, La Jolla, CA). RNA was quantitated with RiboGreen reagent (Molecular Probes, Eugene, OR). For each GFP+ or GFP− sample, RNA was linearly amplified by alternating rounds of cDNA synthesis and *in vitro* transcription using MessageAmp Kits (Ambion). RNA was labeled using BioArray high-yield RNA transcript labeling kits (Enzo, Farmingdale, NY). Synthesized RNA from each sample was hybridized to a Mouse Genome U74Av2 array (Affymetrix, Santa Clara, CA). Each sample was processed independently and hybridized to a different array. Array results were analyzed using the Microarray Suite software (version 4.0; Affymetrix). All arrays were normalized to the same average intensity on the basis of the hybridization signal of the probe sets corresponding to the 60th-90th percentile. Array data were analyzed using the Teradata relational database and algorithms (TeraGenomics; available at http://www.teragenomics.com). Criteria used to identify probe sets with signal differences between GFP+ and GFP− cells included a consistent call of increased and/or marginally increased or decreased and/or marginally decreased change >1.8-fold, an absolute difference change >50 in at least six of the nine comparisons and a present call in at least one of the comparison files. To approximate the false positive rate for this analysis, we applied the same criteria independently to comparisons between individual GFP+ or GFP− samples.

Results

Chromosome displacement and aneuploidy among mitotic SVZ cells *in vivo*

Chromosome displacement, postulated to contribute to CNS aneuploidy in the developing cerebral cortex (Rehen et al., 2001), was identified among proliferating cells of the postnatal SVZ. Twenty micrometer sections of P5 SVZ were immunostained for phosphorylated histone H3 (phospho-H3) to label the condensed chromosomes of cells in M-phase (Hendzel et al., 1997; Rehen et al., 2001) (Fig. 1*B*). In 7% of cells examined, chromosomes were displaced from the main metaphase plate (Fig. 1*C*), suggesting that some SVZ cells mis-segregate their chromosomes.

The predicted result of chromosome mis-segregation is aneuploidy. Rates of aneuploidy in the SVZ were determined by examination of metaphase chromosome spreads isolated from P5–P10 mice (Fig. 1*D*) as described previously (Barch et al., 1997; Rehen et al., 2001). Karyotyping of such spreads by staining with 4′6′-diamidino-2-phenylindole hydrochloride (DAPI) or SKY (Liyanage et al., 1996) provides an accurate estimate of chromosome number in neural cells (Rehen et al., 2001). DAPI staining (Fig. 1*E*,*F*) and SKY of 65 chromosome spreads from P5–P10 SVZ revealed frequent numerical, but not structural, chromosomal abnormalities in these cells. In contrast, karyotype abnormalities were rarely seen in stimulated peripheral lymphocytes, a standard cytogenetic control preparation (data not shown) (Rehen et al., 2001). The normal number of chromosomes in a diploid mouse cell is 40. One-third (33%) of cells from the postnatal SVZ did not have 40 chromosomes (Fig. 1*G*). A strong bias toward chromosome loss existed among aneuploid cells: ~25% had fewer than 40 chromosomes. Importantly, a majority of aneuploid cells was missing multiple chromosomes.

To additionally characterize the incidence of mosaic aneuploidy among normal somatic cells, we karyotyped mitotic cells from the livers of E13 mice. Among 48 mitotic liver cells karyotyped by SKY or DAPI staining, five (10.42%) were aneuploid (data not shown). This rate of aneuploidy was significantly lower than that seen among P5–P10 SVZ cells ($p < 0.01$; χ^2) but was not significantly different from the rate seen among peripheral lymphocytes (3.4%), suggesting that the rates of mosaic aneuploidy are higher in the CNS than in other tissues.

Aneuploidy among interphase SVZ and postnatal-born olfactory bulb cells *in vivo*

To confirm that many SVZ cells were aneuploid, we harvested nuclei from male P5–P10 SVZ and counted their sex chromo-

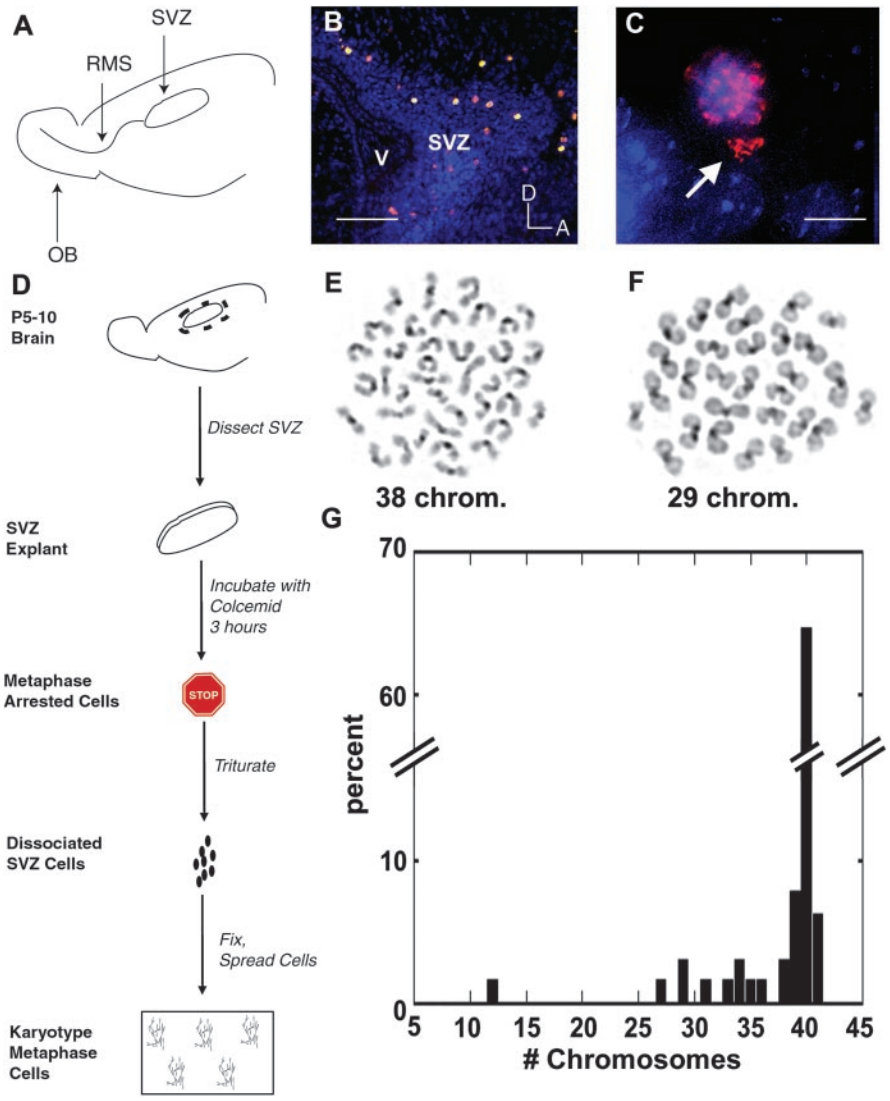

Figure 1. Chromosome displacement and aneuploidy in the SVZ. *A*, Schematic parasaggital view of P5 brain depicting the SVZ, RMS, and OB. *B*, Low power (20×) view of a parasaggital section of P5 SVZ stained with anti-phospho-H3 antibody (red) and DAPI (blue). Note the concentration of phospho-H3 positive mitotic cells in the SVZ. Scale bar, ~50 μm. V, Lateral ventricle; D, dorsal; A, anterior. *C*, High power (100×) view of a single phospho-H3-positive cell (red) with displaced chromosomes (arrow). Note the displaced chromosomes stain with both DAPI and phospho-H3. Scale bar, ~5 μm. *D*, Schematic SVZ karyotyping protocol. After dissection, SVZ explants are incubated with colcemid for 3 hr before dissociation and fixation. *E*, *F*, DAPI-stained aneuploid metaphase chromosome spreads. The cell in *E* has 38 chromosomes; the cell in *F* has 29. A euploid cell in the mouse has 40 chromosomes. *G*, Chromosome number histogram for 65 karyotyped metaphase cells (66% of cells karyotyped were euploid). Of aneuploid cells, the majority lost one or more chromosomes.

Table 1. Sex chromosome loss and gain among SVZ and OB cells

	XY (%)	XO (%)	OY (%)	XXY (%)	XYY (%)	Total abnormal (%)
Adult olfactory bulb	95.67	3.54	0.39	0	0.39	4.33
Postnatal SVZ	95	5	0	0	0	5
Postnatal-born OB	94.03	2.24	0.75	2.24	0.75	5.97
SVZ neurons *in vitro*	91.03	7.62	0.45	0.9	0	8.97
SVZ glia *in vitro*	93.53	2.99	1.49	1	1	6.47
SVZ NPCs *in vitro*	92.24	3.67	1.63	1.63	0.82	7.76

somes by interphase FISH with chromosome paints for mouse X and Y chromosomes (XY FISH) (Rehen et al., 2001). On the basis of karyotyping of mitotic SVZ cells and previous measurements of sex chromosome gain and loss among proliferating embryonic neuronal progenitors, 6–8% of SVZ nuclei were expected to have lost a sex chromosome. XY FISH measurement revealed 5% of cells examined had lost an X or Y chromosome (Table 1, postnatal SVZ), a rate near that measured for proliferating neuronal progenitor cells of the embryonic cerebral cortex (Rehen et al., 2001) and substantially above the false positive rate for this assay (< 2%). XY FISH and karyotyping of metaphase chromosome spreads require different methods for sample preparation and capture cells in different stages of cell-cycle progression, yet the two techniques yielded complementary results. This demonstrated that some SVZ cells were aneuploid.

The substantial rate of aneuploidy among proliferating SVZ cells prompted us to ask whether aneuploidy persists in SVZ-born cells that migrate to the olfactory bulb. Aneuploidy was examined among OB neurons that are born in the postnatal SVZ and migrate to the granular and periglomerular layers of the OB through the rostral migratory stream (Lois and Alvarez-Buylla, 1994; Craig et al., 1999). These cells were identified by injecting 7-d-old male mice with bromodeoxyuridine (BrdU) (Fig. 2*A*). Eight days after injection, cell nuclei from the OB were harvested, processed for XY FISH, and immunostained for BrdU (Fig. 2*A*). In the OB, 5.97% of BrdU-positive cells lost or gained a sex chromosome (Fig. 2*B*; Table 1, postnatal-born OB), a rate slightly higher than that observed in all OB cells (4.33%) (Table 1, adult olfactory bulb). These results suggest that some of the aneuploid cells born in the SVZ are competent to migrate and survive as neurons in the OB.

Aneuploidy among the major SVZ cell types *in vitro*

What SVZ cell types are aneuploid? The SVZ is an especially useful preparation for determining the identities of aneuploid cells on the basis of previous studies that have categorized neurons, glia, and NPCs by immunohistochemistry and ultrastructure (Doetsch et al., 1997). Each cell type can also be cultured and purified *in vitro* (Reynolds et al., 1992; Lim and Alvarez-Buylla, 1999). To this end, P5–P10 SVZ cells were grown in media with serum for 5–10 d and microtobule-associated protein 2 (MAP-2) immunoreactive neurons (Fig. 3*C*) or glial fibrillary acidic protein (GFAP) immunoreactive (Fig. 3*E*) glial cells were isolated by the method of Lim and Alvarez-Buylla (1999). Alternatively, SVZ cells were grown without serum and with 20 ng/ml of EGF and 10 ng/ml of FGF-2 for 5–10 d to generate cultures highly enriched for stem and progenitor cells (Reynolds et al., 1992; Craig et al., 1996). XY FISH revealed that

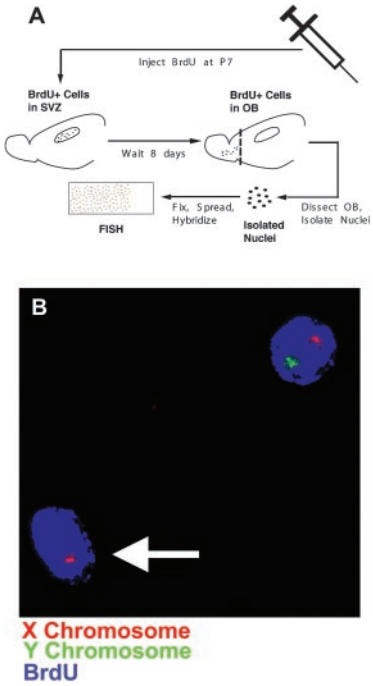

Figure 2. Migration of aneuploid cells to the olfactory bulb. *A*, Schematic experimental protocol. Male P7 mice were given a single intraperitoneal injection of BrdU and survived for 8 d before isolation of nuclei from the OB for FISH and BrdU detection. *B*, Examples of BrdU-positive euploid and aneuploid nuclei. FISH probes paint X (red) and Y (green) chromosomes. The BrdU+ cell in the bottom left (arrow) lost the Y chromosome, whereas the BrdU+ cell in the top right has both an X and a Y.

6–9% of cells of each type had gained or lost a sex chromosome (Fig. *3B–F*; Table 1, SVZ neurons, glia, NPCs *in vitro*). Similar results were obtained when cells were hybridized with whole chromosome 14 paints (data not shown). These results demonstrated that aneuploidy was common to multiple CNS cell types. Given that the majority of dividing cells in the SVZ are progenitor cells (Doetsch et al., 2002), which in turn arise from glia-like stem cells (Doetsch et al., 1999), these results strongly suggest that chromosomal changes in NPCs are propagated to neurons *in vivo*.

Losses of heterozygosity in aneuploid SVZ cells *in vitro* and *in vivo*

One possible functional consequence of aneuploidy is altered gene expression in cells of the SVZ and OB. Given the preponderance of chromosome loss among aneuploid cells, many SVZ and OB cells likely harbor multiple losses of heterozygosity (Lengauer et al., 1998; Serra et al., 2001; Thiagalingam et al., 2002). Although normal diploid cells have two copies of each autosome, many aneuploid cells in the SVZ and OB have only one copy of at least one autosome. In these cells, loss of heterozygosity (LOH) would abolish expression of alleles on lost chromosomes, allowing only expression of alleles present on remaining ones.

This possibility was examined in a model system that captured the essential features of LOH: loss of expression of a globally expressed hemizygous transgene. We analyzed mice hemizygous for an enhanced green fluorescent protein (eGFP) transgene driven by the chick β-actin promoter (Okabe et al., 1997) and present at a single locus on chromosome 15 (Fig. 4*A* and data not shown). These mice were chosen because cells possessing the transgene express it constitutively at a high level (Okabe et al., 1997), and because the transgene is expressed by >90% of CNS cells (Fig. 5*A*). SVZ cells from these mice were cultured and analyzed for GFP fluorescence and chromosome 15 copy number. Approximately 25% of cultured SVZ cells appeared to not express the transgene (Fig. 4*B*,*C*). Among these cells, 23% had also lost one copy of chromosome 15 (Fig. 4, box 1). In contrast, 96% of GFP+ cells had two copies of chromosome 15 (Fig. 4, box 2), suggesting that loss of one copy of chromosome 15, most likely the copy carrying the eGFP transgene, had caused loss of eGFP expression through a mechanism similar to LOH.

Chromosome loss was also identified as a source of LOH *in vivo*. Acutely isolated SVZ or OB cells were separated on the basis of GFP expression by FACS, resulting in purified GFP+ and GFP− cells (Figs. 5*A*, 6*A*,*B*). For this analysis, GFP− cells were those with a GFP fluorescence peak area that was two SDs less than the mean for all cells (i.e., the 2% of cells with the least fluorescence). FISH for chromosome 15 identified 45–50% of GFP− cells in the SVZ and OB that had lost a copy of chromosome 15 (Fig. 5*B*). In contrast, only 2–12% of GFP+ cells lost a copy of 15, which reflected a loss of the nontransgenic copy of chromosome 15, because these cells were derived from mice with a hemizygous eGFP genotype.

To confirm loss of the copy of chromosome 15 carrying the eGFP transgene among GFP− cells, genomic DNA was taken from GFP+ and GFP− cells isolated by FACS from whole P2–P4 mouse brains and analyzed by semiquantitative genomic PCR for the eGFP transgene and the *s1p3/lpb3/edg3* gene, a control gene present on chromosome 13 (Ishii et al., 2001, 2002). We found that the eGFP transgene was ~90% less abundant relative to *s1p3* in GFP− cells compared with GFP+ cells (Fig. 5*C*). These results were obtained with multiple primer sets and sample replicates (data not shown). Together with the increased rate of chromosome loss among GFP− cells, this finding demonstrates that loss of eGFP expression in some CNS cells is caused by loss of the copy of chromosome 15 carrying the eGFP transgene *in vivo*.

Alteration of gene expression among cells with LOH at chromosome 15

Does chromosome loss alter expression of endogenous genes? To address this question, we harvested RNA from sorted GFP+ and GFP− SVZ cells and used oligonucleotide arrays to generate gene expression profiles of sorted cells and identify differentially expressed genes. To isolate the direct effects of LOH at chromosome 15, cultures of glia and glial-restricted NPCs (Levison and Goldman, 1997) expanded for 10 d *in vitro* were used. Use of these cultures rather than mixed cultures of neurons and glia allowed us to isolate effects of chromosome loss in a single cell type without the complication of potential differences in chromosome 15 loss rates, gene expression programs, or flow-cytometric parameters between neurons and glia. Among GFP+ and GFP− glial cells, gene expression profiling revealed differential expression of 22 genes (Table 2), including both downregulated and upregulated genes on several different chromosomes (data not shown). These data demonstrate that endogenous gene expression programs are altered by loss of chromosome 15, and such changes are not limited to the lost chromosome.

Proliferation and survival of cells with LOH at chromosome 15

To determine whether LOH at chromosome 15 affects the proliferation or survival of glial cells, we stained sorted SVZ glial cells for a marker of proliferation, phosphorylated-vimentin (A4A; phospho-Ser55-vimentin) (Tsujimura et al., 1994; Kamei et al., 1998), or cell death (cleaved caspase-3) (Pompeiano et al., 2000). SVZ glia and glial-restricted NPCs (Levison and Goldman, 1997)

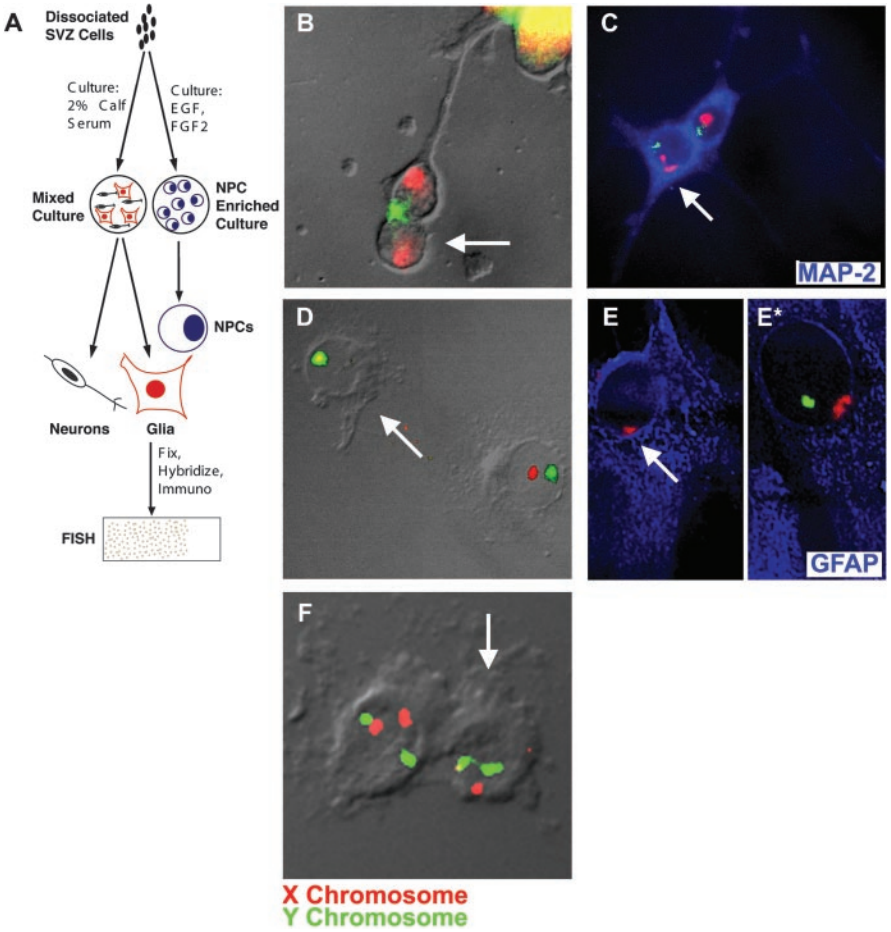

Figure 3. Aneuploidy among NPCs and their progeny *in vitro*. *A*, Schematic experimental protocol. SVZ cells were harvested from P5–P10 mice, cultured with 2% fetal calf serum or 20 ng/ml of EGF and 10 ng/ml of FGF-2 for 5–10 d before harvesting specific cell types using established methods. *B*, *D*, *F*, Nomarski and X (red) and Y (green) FISH images of cultured SVZ cells. *C*, *E*, Antibody-stained (blue) and X (red) and Y (green) FISH images of cultured SVZ cells. *B*, An SVZ-generated neuron without a Y chromosome (arrow). Note that the cell above it has both X and Y. *C*, An SVZ-generated, MAP-2-expressing neuron (blue) with two X chromosomes and one Y chromosome (arrow). The adjacent neuron is euploid. *D*, An SVZ-generated glial cell with no X chromosome (arrow). The cell in the bottom right is euploid. *E*, An SVZ-generated, GFAP immunoreactive glial cell (blue) that lost a Y chromosome (arrow). Note the glial cell in the adjacent panel *E** is euploid. *F*, An aneuploid NPC (arrow) with one X chromosome and two Y chromosomes. The cell on the left has two X and two Y chromosomes, suggesting it is tetraploid.

were expanded for 10 d before FACS sorting and plating on cell-tak-coated coverslips. Similar rates of vimentin phosphorylation (Fig. 6*G*) and caspase-3 cleavage (Fig. 6*H*) were observed among both GFP+ and GFP− cells, suggesting that LOH at chromosome 15 alone does not exert a strong effect on proliferation or survival of glia or glia-restricted NPCs. However, these data suggest that cells in the glial lineage with LOH at chromosome 15 are competent to divide and survive at essentially normal rates *in vitro*.

Discussion

Mosaic aneuploidy in the postnatal SVZ and OB

This study focused on aneuploidy and its consequences for neural cells. In the postnatal SVZ (a germinal region) and OB (a site of incorporation of postnatally born cells), many neurons, glia, and NPCs were found to be aneuploid. We propose that aneuploidy first arises in NPCs during mitosis, an idea that is consistent with previous work in the embryonic cortex (Rehen et al., 2001).

A likely fate for many aneuploid SVZ cells is death, given the high rates of apoptosis observed among postnatally born neurons in the rostral migratory stream (RMS) and OB (Morshead and van der Kooy, 1992). However, many BrdU-labeled aneuploid cells were found in the OB, and the rate of caspase-3 cleavage was not significantly elevated among cells with LOH on chromosome 15. These findings strongly suggest that some aneuploid cells produced in the SVZ migrate and survive within the OB as postmitotic neurons, also consistent with previous studies on the adult cerebral cortex (Rehen et al., 2001). Together, data from the SVZ and OB may be interpreted to mean that genetic diversity is generated among proliferating cells in the SVZ and persists among OB neurons.

High rates of chromosome loss among interphase cells

In this study, the rates of loss of both autosomes and sex chromosomes in interphase SVZ and OB cells fell in the range of 2–8% (Table 2). It is important to consider these rates in the context of metaphase karyotypes. For example, if the loss rates observed for sex chromosomes and chromosome 15 in SVZ and OB cells are representative of all chromosomes, we would predict that 100% of cells would be missing one chromosome, which is clearly not the case. This difficulty is resolved by the fact that, among metaphase SVZ cells (Fig. 1*G*), ~8% lost only one chromosome, whereas ~17% lost multiple chromosomes.

Comparison of the rates of chromosome loss from metaphase and interphase cells provides a mechanism for cross-checking the accuracy of these measurements. On the basis of data from metaphase spreads, the average number of chromosomes among SVZ cells is 38.75 chromosomes per cell, suggesting an average chromosome loss rate of 5.13%. For all observations of sex chromosome loss among interphase cells, the average chromosome loss rate was 4.96%, leading to an average chromosome number estimate of 39.08, in agreement with the estimates from metaphase cells. This suggests that both interphase and metaphase estimates of chromosome loss rates in the SVZ are accurate (within 0.2% of one another) and in accord with previous data that establish the accuracy of these measurements in the cerebral cortex (Rehen et al., 2001).

Loss of heterozygosity and alteration of gene expression by chromosome loss

The functional consequences of neural cell aneuploidy have not been examined previously. Here, we have shown that chromosome loss among normal neural cells can cause LOH and, in turn, alter gene expression profiles, in line with previous results from tumor models and yeast (Hughes et al., 2000; Phillips et al., 2001). However, we note the possibility that upregulation or downregulation of some genes may be caused indirectly by other differences between GFP+ and GFP− cells such as altered GFP expression levels.

Differentially expressed genes provide clues to the possible functional consequences of chromosome loss. For example, three

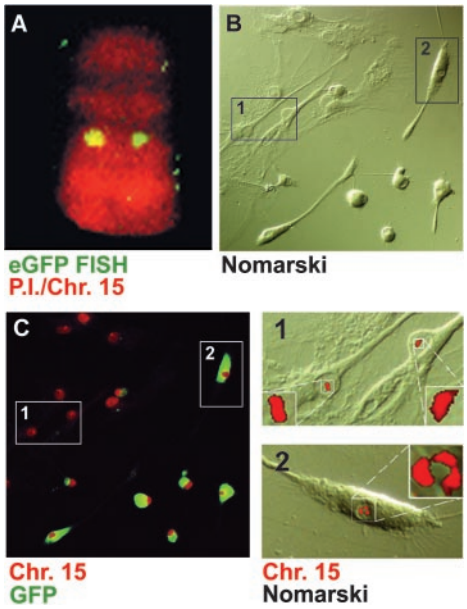

Figure 4. Chromosome 15 loss is reported by loss of transgene expression *in vitro*. *A*, FISH detects an eGFP transgene integrated at a single locus on chromosome 15. (Two hybridization signals are visible in this chromatid pair.) eGFP expression is driven by the chicken β-actin promoter and cytomegalovirus enhancer; a high level of expression is expected in all cells in which the transgene is present. Subsequent analyses were performed in eGFP hemizygotes. *B*, *C*, Variation in eGFP fluorescence in SVZ cells *in vitro*. *B* is a Nomarski image and *C* shows eGFP fluorescence (green) and chromosome 15 FISH (red). Cells in boxes 1 (GFP−) and 2 (GFP+) are enlarged in adjacent panels. Boxes 1 and 2, GFP− cells frequently have only one copy of chromosome 15 (red). Cells in box 1 are GFP− and have only one copy of chromosome 15. The cell in box 2 is GFP+ and has two copies of 15.

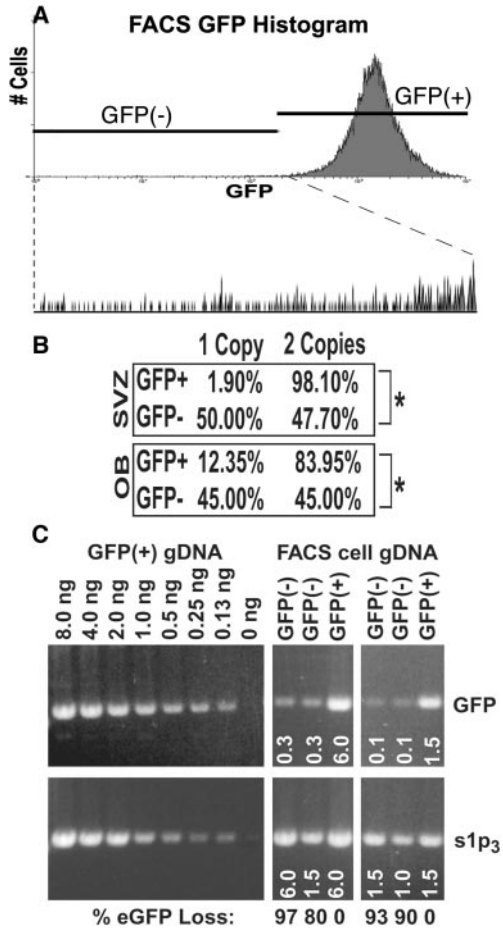

Figure 5. Chromosome 15 loss is a significant source of LOH *in vivo*. *A*, GFP fluorescence histogram from FACS sorting of P5 SVZ. Note that ~2% of cells have very little GFP fluorescence (expanded view below). Similar results were obtained with OB cells (data not shown). *B*, Quantitation of chromosome 15 loss and gain among GFP+ and GFP− sorted cells from P5 SVZ and OB. Forty-five to fifty percent of GFP− cells have one copy of chromosome 15, whereas 88–98% of GFP+ cells have two copies. GFP+ and GFP− distributions from both SVZ and OB are significantly different from one another (*$p < 0.00001$; χ^2 test). *C*, Ethidium bromide-stained gel showing PCR-amplified eGFP (chromosome 15) or s1p3 (chromosome 13). Known amounts of gDNA from tail tissue (left panels) were used as a standard for estimating template quantities. In the experimental samples (right panels), the template was gDNA from FACS-sorted GFP+ or GFP− brain cells. The estimated template gDNA quantities are indicated below the amplified fragments (ng). On the basis of these numbers, the percentage of eGFP loss in the samples was determined and is listed below each lane. Experimental sample determinations were repeated >8 times (also with distinct primer pairs for GFP and another control gene, s1p2), and the percentage of GFP loss averaged ~90%.

differentially expressed genes are known to be involved in Ca^{2+} signal transduction: *annexin A1*, *calpain small subunit 1*, and *ata2* (Perlmutter et al., 1988; Gerke and Moss, 1997). Of these, *ata2* expression is increased threefold (3.02×), possibly to compensate for decreased expression of *annexin A1* (−3.2×) and *calpain small subunit 1* (−1.89×).

Despite these alterations of gene expression, proliferation and survival of cells with LOH at chromosome 15 was essentially normal. This suggests that aneuploid stem and progenitor cells may produce aneuploid neurons and glia at rates near those of euploid cells. However, there may be differences in the long-term viability of differentiated aneuploid SVZ cells relative to euploid ones. Along similar lines, the functional consequences of chromosome loss may be more pronounced in differentiated or stressed cells.

The loss of a chromosome is typically lethal to organisms (Miller and Therman, 2001). However, our data suggest that although chromosome loss does lead to haploinsufficiency and altered gene expression programs in SVZ cells, such changes are not necessarily lethal. Why not? Progress toward understanding the teleological causes and effects of chromosome loss in neural cells will likely be aided by studies of computer models of gene networks. Such models are useful tools for understanding the robustness or fragility of networks of cells and genes over evolutionary time (von Dassow et al., 2000) and can be adapted to study the effects of mosaic aneuploidy in gene networks of neurobiological interest.

Evidence for subchromosomal genomic alterations in SVZ cells

Among GFP− cells, the rate of depletion of the eGFP transgene (~90%) exceeded the rate of loss of chromosome 15 carrying the transgene (~50%). This disparity may reflect a high rate of deletions (~40% among cells that lose GFP expression) that encompass the eGFP transgene but not the entire copy of chromosome 15. We speculate that similar alterations to other chromosomes may be present in many CNS cells and other genomic alterations may also occur on the backdrop of mosaic aneuploidy in the CNS, as suggested by the functions of DNA modifying and/or surveillance factors during neuronal development (Gao et al., 1998; Chun and Schatz, 1999a, b; Allen et al., 2001).

Future directions

This work demonstrates that chromosome loss produces permanent genomic changes in normal neural cells of the SVZ and OB, and such changes can alter gene expression in morphologically normal cells. However, our studies have not addressed the effects

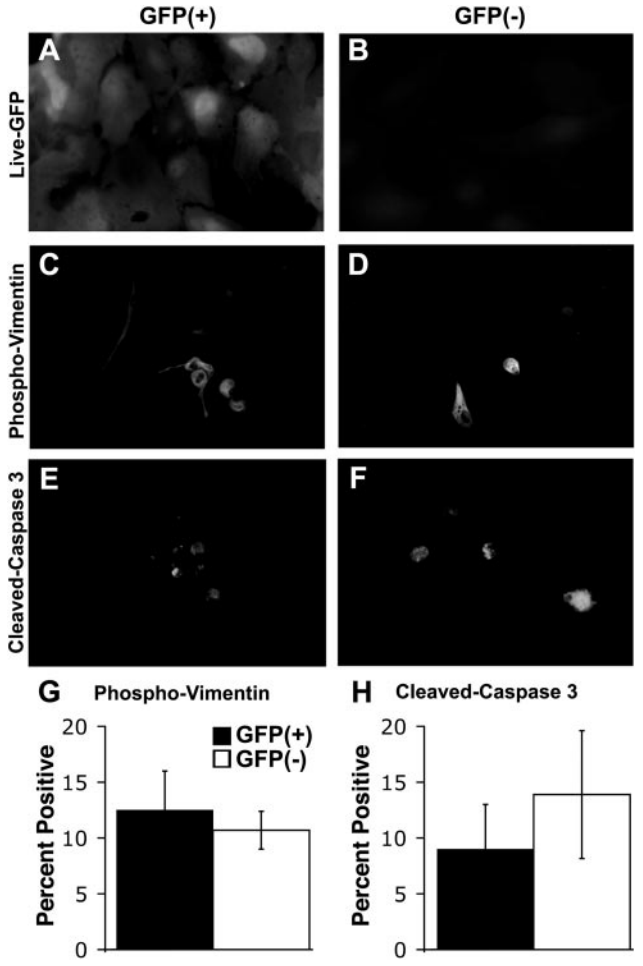

Figure 6. Proliferation and survival of cells with LOH at chromosome 15 *in vitro*. *A*, *B*, Representative 40× micrographs of GFP fluorescence among live FACS-sorted GFP+ (*A*) and GFP− (*B*) cells 24 hr after sorting. Images in each row (*A–B*, *C–D*, *E–F*) were captured using identical exposure and camera gain settings and depict areas with similar cell densities. Note that cells in the GFP− culture are clearly less fluorescent than GFP+ cells. *C*, *D*, Representative 20× micrographs of phospho-vimentin antibody staining of GFP+ (*C*) and GFP− (*D*) cells 24 hr after sorting. *E*, *F*, Representative 20× micrographs of cleaved caspase-3 staining of GFP+ (*E*) and GFP[mnus] (*F*) cells 24 hr after sorting. *G*, No change in rates of vimentin phosphorylation among GFP− cells relative to GFP+. The percentage of cells immunoreactive for phospho-vimentin is presented as mean ± SE.

of increased chromosomal copy number (hyperploidy) (Rehen et al., 2001), nor the effects of more complex karyotype abnormalities such as the co-existence of chromosome gain and loss in a single cell. Similarly, subtle or indirect consequences of LOH via "trans" effects (transcription and signaling factors) or other extragenic modifiers (Hamilton et al., 1997) were not addressed, although we note the possibility of such effects through LOH. LOH among neural cells could unmask recessive traits (via dominant allele loss), which could not be rescued by gene amplification or chromosome gain. Scientific understanding of the effects of mosaic aneuploidy on normal brain function and pathology will benefit from a focus on these issues in future studies.

Table 2. Differential expression of genes in GFP+ and GFP− cells

Gene name	Fold change expression*
Expressed sequence AI852726	3.47
Expressed sequence AI552542	3.1
ATA2	3.02
IMAGE clone 990720	2.59
Ribosomal protein L36	2.56
RW1	2.55
ESTs, weakly similar to solute carrier family 4	2.36
Expressed sequence AA536743	2.26
IMAGE clone 3994696	2.2
Expressed sequence AA682085	2.17
Hydroxysteroid (17β) dehydrogenase 12	1.91
RIKEN cDNA 5430432P15	1.84
IMAGE clone 4019917	1.77
cDNA sequence BC033609	1.63
Gene rich cluster, C9 gene	−1.87
Calpain, small subunit 1	−1.89
Phosphoprotein enriched in astrocytes 15	−1.93
Dscr28C related cytoplasmic tyrosine kinase	−2.62
Thymus cell antigen 1, θ	−2.65
N-myc downstream regulated-like	−3.12
Annexin A1	−3.19
Stathmin-like 2	−3.68

* Expressed relative to paired GFP+ samples.

References

Aboody KS, Brown A, Rainov NG, Bower KA, Liu S, Yang W, Small JE, Herrlinger U, Ourednik V, Black PM, Breakefield XO, Snyder EY (2000) Neural stem cells display extensive tropism for pathology in adult brain: evidence from intracranial gliomas. Proc Natl Acad Sci USA 97:12846–12851.

Allen DM, van Praag H, Ray J, Weaver Z, Winrow CJ, Carter TA, Braquet R, Harrington E, Ried T, Brown KD, Gage FH, Barlow C (2001) Ataxia telangiectasia mutated is essential during adult neurogenesis. Genes Dev 15:554–566.

Alvarez-Buylla A, Garcia-Verdugo JM (2002) Neurogenesis in adult subventricular zone. J Neurosci 22:629–634.

Barch MJ, Knudsen T, Spurbeck JL (1997) The AGT cytogenetics laboratory manual, Chap 3, Ed 3. Philadelphia: Lippincott–Raven.

Chun J, Schatz DG (1999a) Developmental neurobiology: alternative ends for a familiar story? Curr Biol 9:R251–R253.

Chun J, Schatz DG (1999b) Rearranging views on neurogenesis: neuronal death in the absence of DNA end-joining proteins. Neuron 22:7–10.

Craig CG, Tropepe V, Morshead CM, Reynolds BA, Weiss S, van der Kooy D (1996) *In vivo* growth factor expansion of endogenous subependymal neural precursor cell populations in the adult mouse brain. J Neurosci 16:2649–2658.

Craig CG, D'sa R, Morshead CM, Roach A, van der Kooy D (1999) Migrational analysis of the constitutively proliferating subependyma population in adult mouse forebrain. Neuroscience 93:1197–1206.

Doetsch F, Garcia-Verdugo JM, Alvarez-Buylla A (1997) Cellular composition and three-dimensional organization of the subventricular germinal zone in the adult mammalian brain. J Neurosci 17:5046–5061.

Doetsch F, Caille I, Lim DA, Garcia-Verdugo JM, Alvarez-Buylla A (1999) Subventricular zone astrocytes are neural stem cells in the adult mammalian brain. Cell 97:703–716.

Doetsch F, Verdugo JM, Caille I, Alvarez-Buylla A, Chao MV, Casaccia-Bonnefil P (2002) Lack of the cell-cycle inhibitor p27Kip1 results in selective increase of transit-amplifying cells for adult neurogenesis. J Neurosci 22:2255–2264.

Fukushima N, Kimura Y, Chun J (1998) A single receptor encoded by *vzg-1/lp$_{A1}$/edg-2* couples to G proteins and mediates multiple cellular responses to lysophosphatidic acid. Proc Natl Acad Sci USA 95:6151–6156.

Gage FH (2002) Neurogenesis in the adult brain. J Neurosci 22:612–613.

Gao Y, Sun Y, Frank KM, Dikkes P, Fujiwara Y, Seidl KJ, Sekiguchi JM, Rathbun GA, Swat W, Wang J, Bronson RT, Malynn BA, Bryans M, Zhu C, Chaudhuri J, Davidson L, Ferrini R, Stamato T, Orkin SH, Greenberg ME, Alt FW (1998) A critical role for DNA end-joining proteins in both lymphogenesis and neurogenesis. Cell 95:891–902.

Gerke V, Moss SE (1997) Annexins and membrane dynamics. Biochim Biophys Acta 1357:129–154.

Hamilton BA, Smith DJ, Mueller KL, Kerrebrock AW, Bronson RT, van Berkel V, Daly MJ, Kruglyak L, Reeve MP, Nemhauser JL, Hawkins TL, Rubin EM, Lander ES (1997) The vibrator mutation causes neurodegeneration via reduced expression of PITP alpha: positional complementation cloning and extragenic suppression. Neuron 18:711–722.

Hendzel MJ, Wei Y, Mancini MA, Van Hooser A, Ranalli T, Brinkley BR, Bazett-Jones DP, Allis CD (1997) Mitosis-specific phosphorylation of histone H3 initiates primarily within pericentromeric heterochromatin during G2 and spreads in an ordered fashion coincident with mitotic chromosome condensation. Chromosoma 106:348–360.

Hughes TR, Roberts CJ, Dai H, Jones AR, Meyer MR, Slade D, Burchard J, Dow S, Ward TR, Kidd MJ, Friend SH, Marton MJ (2000) Widespread aneuploidy revealed by DNA microarray expression profiling. Nat Genet 25:333–337.

Ishii I, Friedman B, Ye X, Kawamura S, McGiffert C, Contos JJ, Kingsbury MA, Zhang G, Brown JH, Chun J (2001) Selective loss of sphingosine 1-phosphate signaling with no obvious phenotypic abnormality in mice lacking its G protein-coupled receptor, LP(B3)/EDG-3. J Biol Chem 276:33697–33704.

Ishii I, Ye X, Friedman B, Kawamura S, Contos JJ, Kingsbury MA, Yang AH, Zhang G, Brown JH, Chun J (2002) Marked perinatal lethality and cellular signaling deficits in mice null for the two sphingosine 1-phosphate receptors, S1P2/LPB2/EDG-5 and S1P3/LPB3/EDG-3. J Biol Chem 277:25152–25159.

Kamei Y, Inagaki N, Nishizawa M, Tsutsumi O, Taketani Y, Inagaki M (1998) Visualization of mitotic radial glial lineage cells in the developing rat brain by Cdc2 kinase-phosphorylated vimentin. Glia 23:191–199.

Kawakami N, Sakane N, Nishizawa F, Iwao M, Fukada SI, Tsujikawa K, Kohama Y, Ikawa M, Okabe M, Yamamoto H (1999) Green fluorescent protein-transgenic mice: immune functions and their application to studies of lymphocyte development. Immunol Lett 70:165–171.

Lengauer C, Kinzler KW, Vogelstein B (1998) Genetic instabilities in human cancers. Nature 396:643–649.

Levison SW, Goldman JE (1997) Multipotential and lineage restricted precursors coexist in the mammalian perinatal subventricular zone. J Neurosci Res 48:83–94.

Lim DA, Alvarez-Buylla A (1999) Interaction between astrocytes and adult subventricular zone precursors stimulates neurogenesis. Proc Natl Acad Sci USA 96:7526–7531.

Liyanage M, Coleman A, du Manoir S, Veldman T, McCormack S, Dickson RB, Barlow C, Wynshaw-Boris A, Janz S, Wienberg J, Ferguson-Smith MA, Schrock E, Ried T (1996) Multicolour spectral karyotyping of mouse chromosomes. Nat Genet 14:312–315.

Lois C, Alvarez-Buylla A (1994) Long-distance neuronal migration in the adult mammalian brain. Science 264:1145–1148.

Miller OJ, Therman E (2001) Human chromosomes, Ed 4, p 183. New York: Springer.

Morshead CM, van der Kooy D (1992) Postmitotic death is the fate of constitutively proliferating cells in the subependymal layer of the adult mouse brain. J Neurosci 12:249–256.

Okabe M, Ikawa M, Kominami K, Nakanishi T, Nishimune Y (1997) "Green mice" as a source of ubiquitous green cells. FEBS Lett 407:313–319.

Perlmutter LS, Siman R, Gall C, Seubert P, Baudry M, Lynch G (1988) The ultrastructural localization of calcium-activated protease "calpain" in rat brain. Synapse 2:79–88.

Phillips JL, Hayward SW, Wang Y, Vasselli J, Pavlovich C, Padilla-Nash H, Pezullo JR, Ghadimi BM, Grossfeld GD, Rivera A, Linehan WM, Cunha GR, Ried T (2001) The consequences of chromosomal aneuploidy on gene expression profiles in a cell line model for prostate carcinogenesis. Cancer Res 61:8143–8149.

Pompeiano M, Blaschke AJ, Flavell RA, Srinivasan A, Chun J (2000) Decreased apoptosis in proliferative and postmitotic regions of the Caspase 3-deficient embryonic central nervous system. J Comp Neurol 423:1–12.

Rehen SK, McConnell MJ, Kaushal D, Kingsbury MA, Yang AH, Chun J (2001) Chromosomal variation in neurons of the developing and adult mammalian nervous system. Proc Natl Acad Sci USA 98:13361–13366.

Reynolds BA, Tetzlaff W, Weiss S (1992) A multipotent EGF-responsive striatal embryonic progenitor cell produces neurons and astrocytes. J Neurosci 12:4565–4574.

Serra E, Rosenbaum T, Nadal M, Winner U, Ars E, Estivill X, Lazaro C (2001) Mitotic recombination effects homozygosity for NF1 germline mutations in neurofibromas. Nat Genet 28:294–296.

Thiagalingam S, Foy RL, Cheng KH, Lee HJ, Thiagalingam A, Ponte JF (2002) Loss of heterozygosity as a predictor to map tumor suppressor genes in cancer: molecular basis of its occurrence. Curr Opin Oncol 14:65–72.

Tsujimura K, Ogawara M, Takeuchi Y, Imajoh-Ohmi S, Ha MH, Inagaki M (1994) Visualization and function of vimentin phosphorylation by cdc2 kinase during mitosis. J Biol Chem 269:31097–31106.

von Dassow G, Meir E, Munro EM, Odell GM (2000) The segment polarity network is a robust developmental module. Nature 406:188–192.